NASA Technical Memorandum 102005

Advanced Computational Techniques for Hypersonic Propulsion

Louis A. Povinelli
Lewis Research Center
Cleveland, Ohio

Prepared for the
9th International Symposium on Air Breathing Engines
cosponsored by the American Institute of Aeronautics and Astronautics
and the International Society for Air Breathing Engines
Athens, Greece, September 4–9, 1989

NASA

ADVANCED COMPUTATIONAL TECHNIQUES FOR HYPERSONIC PROPULSION

Louis A. Povinelli*
National Aeronautics and Space Administration
Lewis Research Center
Cleveland, Ohio 44135

Abstract

CFD has played a major role in the resurgence of hypersonic flight, on the premise that numerical methods will allow us to perform simulations at conditions for which no ground test capability exists. Validation of CFD methods is being established using the experimental data base available, which is below Mach 8. It is important, however, to realize the limitations involved in the extrapolation process as well as the deficiencies that exist in numerical methods at the present time. Current features of CFD codes are examined for application to propulsion system components. The shortcomings in simulation and modeling are identified and discussed.

Introduction

An overwhelming degree of reliance has been placed on computational fluid dynamics in the achievement of hypersonic flight with a NASP-like vehicle (National Aero-Space Plane Program). This reliance covers the range of design activities; from the design of the aircraft configuration to the design of the integrated engine system. The belief that CFD can be used to predict all of the relevant flow physics and chemistry, from aircraft takeoff to orbital speeds and return, has been one of the principal reasons for the resurgence of hypersonic research.[1] Computational methods do, in fact, provide us with the unique ability to perform ground simulations at high Mach numbers for which no ground test capability exists. Above Mach numbers of approximately 8, ground test facilities do not duplicate the relevant flight simulation parameter such as Mach number, Reynolds numbers, gas composition, and enthalpy level. Numerical analysis remains as the principal approach to the design of the aircraft and the propulsion system. It is possible that some data could be obtained from rocket test vehicles. These data would be limited, however to such items as the state of the boundary layer, boundary layer transition location, length of the transition zone and surface heat transfer. Testing of a scramjet propulsion system on a rocket vehicle would present a major problem due to the fact that scaling of the combustion process is not feasible. Therefore, a full sized propulsion module would be required as the test article on a rocket test vehicle. Such testing might be better approached through use of larger vehicles such as the Space Shuttle. However, it is currently believed that the costs associated with the flight testing described above would be extremely high. CFD, therefore, remains as a viable alternative. It must be pointed out that the philosophy regarding CFD is based on the fact that an experimental data base exists below Mach 8. Those data provide the means for assessing the accuracy of the numerical methods, as well as for calibrating the codes. Extrapolation to flight conditions, where no data exists, can then be carried out. In theory, therefore, the procedure described would provide us with ground simulation throughout the Mach number range from takeoff to orbital velocities. It is crucial, however, to realize the capabilities and the limitations involved in the extrapolation process as well as the numerical methods at the present time. In this paper, the current features of the numerical methods available for analyzing the flow in multi-element hypersonic propulsion systems will be presented. Since this paper has as its focus the propulsion system, the aircraft configuration is only discussed relative to the propulsion flow path. Only the integration effects of the forebody and nozzle afterbody configuration will be addressed. Emphasis is placed on the inlet behavior, combustor and nozzle characteristics including ionization and dissociation effects, as well as finite rate and equilibrium chemistry effects. The critical limitations introduced by the need for turbulence, boundary layer transition and chemical modeling are discussed; and the effect of various models is illustrated for the propulsion system components. Shortcomings associated with the extrapolation to higher speeds are also presented. Current and future activities, which are directed toward improving the modeling, are discussed. These activities include elements such as direct numerical simulation, wall and shear layer turbulence modeling and probability density functions for reacting flows.

Propulsion CFD Validation

Hypersonic Propulsion System

In order to demonstrate the ability of CFD codes to perform propulsion system computations and to examine their strengths and their shortcomings, a typical propulsion configuration must be chosen. In this paper, a combined ramjet/scramjet system is assumed which has a common flow path. The low speed or "accelerator" portion of the engine, which would provide sufficient speed for ramjet operation, is not considered here. The assumed flight conditions would correspond to subsonic combustion ramjet operation from flight numbers of approximately Mach 3 up to approximately Mach 5.5, where supersonic combustion operation would commence. Supersonic flow within the engine results in lower temperatures and pressures, thereby reducing heat fluxes and internal forces. The lower temperatures also allow heat to be added from the fuel without imposing high air dissociation losses. However, ignition and combustion of the fuel within the combustor remains a major challenge. The idea of an oblique detonation wave ramjet has been proposed, wherein fuel is injected upstream (inlet) for premixing with air. The mixture is then ignited by a shock wave within the combustor. Detonation wave stability, completeness of combustion and premixing feasibility issues must be solved to understand this concept. In this paper, the detonation engine computations are not considered. Our investigation, therefore, centers on the use of CFD for

*Deputy Chief, Internal Fluid Mechanics Division; Associate Fellow, AIAA.

an integrated airbreathing propulsion system operating at altitudes from near earth to the limits of the stratosphere. In the absence of specific ramjet/scramjet designs, a generic type propulsion system will be used which includes many of the features which are considered important in real systems. Those engine features which cannot be analyzed, for example, complex combustor geometries, will be discussed as limitations of CFD for hypersonic propulsion systems.

The level of sophistication required in the numerical methods varies for each of the system components. For the blunt forebody, a thin layer Navier-Stokes code is required at the nose to handle the strong viscous shock, followed by parabolized Navier-Stokes method to the inlet. Around Mach 7, the vehicle generates a high temperature, high enthalpy flow field. The elevated temperatures in the boundary layers of the vehicle dissociates the oxygen and nitrogen molecules into their respective atomic species which may also become ionized. The process can be catalyzed and enhanced further by vehicle surface contaminants. This dissociation process may lead to variations in local flow-field molecular weight, specific heat and transport properties with resultant associated changes in dynamic airflow, heat transfer and combustor kinetics. These effects cannot be accurately modeled in ground test facilities. Properties of shock heated air and combustion gases are needed for performance predictions. Three-dimensional thin layer or Navier-Stokes are required for the flow in the inlet with the presence of multiple shocks and possible flow separation and unsteadiness. The combustor requires a Navier-Stokes solution including finite rate chemistry as does the nozzle flow field. It is obvious, therefore, that real gas effects, ionization, recombination, nonequilibrium effects, and wall catalyticity must be considered at various locations through the system.

CFD Validation

As mentioned in the Introduction, CFD extrapolation is required for the design of the aircraft/propulsion system at the higher Mach number range ($M > 8$). A critical activity, therefore, is associated with validation/calibration of the numerical techniques. To what extent or level of sophistication is validation required? Must the numerical codes duplicate all of the physics and chemistry in the flow? Before answering these questions, one must be aware of the manner in which codes will be used in the design process. In the case of the inlet, the designer is interested in certain performance parameters such as the amount of mass captured, adiabatic kinetic energy efficiency, pressure recovery, heat load, spillage drag and exit profile. Ideally, then a designer can compute, for a variety of possible inlet geometries over a range of Mach numbers, all of the parameters cited above and, eventually, arrive at a fairly efficient inlet design. At this point, however, it is necessary to ask to what extent is the designer interested in the physical and chemical phenomena occurring in the inlet, such as shock/boundary layer interactions, secondary/corner flows, mass injection, transition, bleed, equilibrium chemistry, flow separation and unsteady flows due to pressure oscillations and shock interactions? The answer is perhaps quite straightforward. The designer is interested in all of the physics and chemistry insofar as it affects the performance parameters cited earlier. If the physical/chemical phenomena do not affect the inlet performance or loadings, it is safe to say that the designer would not be particularly upset if such features were missing in the numerical code.

The relevance of the preceding discussion to the issue of code validation/calibration is that the extent of the validation process and the number of effects to be accounted for are strongly dependent on the magnitude of the individual effects on inlet performance. Another way of stating it is to ask which of the items in the list of physical/chemical phenomena must be modeled by the CFD'er in order for the designer to have valid answers. If none of the items can be ignored, then all of them must be included as the numerical codes are exercised to develop sensitivities to the individual modeling. One must realize that in addition to the modeling required, there are also issues related to the numerics and the math modeling. These issues involve computational grid sensitivity, the ability to capture discontinuities, sensitivity to internal code parameters, the effect of numerical boundary conditions, and conservation of mass, momentum, energy and species. Therefore, one must be concerned with numerical/mathematical modeling as well as physical/chemical modeling. If these activities can be properly executed, then one may proceed to the next stage, which includes the identification of critical experiments and comparison of the numerical results with experimental results. Although the experimental methods will not be discussed, it is equally important to establish the validity and accuracy of the measured data.

The discussion regarding code validation has been somewhat general to this point. To be more specific, Table 1 shows the critical forebody design or performance parameters, the quantities that must be computed by the codes and the physics/chemistry modeling requirements. The same information is shown in Table 2 for the inlet, Table 3 for the combustor and Table 4 for the nozzle. From the viewpoint of a researcher, it is believed that a fundamental understanding of the physics and chemistry within any system must first be understood and then modeled. Its relative importance (and perhaps some eventual control) must first be understood, before a massive sensitivity study (grid, internal parameters) is carried out for every physical or chemical phenomena known to exist in the component. It is proposed, therefore, for CFD validation, that both experimental and numerical research should proceed from the basis of developing understanding first, secondly, making judgments on the importance of various phenomena, and then performing numerical sensitivity studies.

The propulsion system components will be discussed sequentially in the following sections of the paper. The items of special concern are unsteady flow behavior in the inlet, combustion-turbulence modeling in the combustor and shear layer/boundary layer characteristics in nozzle flow.

Numerical Methods for Inlet Flow

Numerical Schemes

Typical results for a high speed inlet will be presented in this section. A fairly significant

number of analyses have been carried out over the last several years at various laboratories (i.e. NASA Lewis, Langley, Rose Engr, APL/JHU). As a means of illustrating the current capability of inlet codes, we consider the results obtained by Benson and co-workers[2-4] using both parabolized and Reynolds averaged Navier-Stokes solvers. The PNS code solves the system of equations for hypersonic or supersonic flow by the linearized block implicit scheme of Briley and McDonald.[5] Since parabolized solvers have inherent limitations regarding separation regions, an approximation is used to allow the code to march through small areas of separated flow. The Reynolds averaged Navier-Stokes code (PARC3D) solves the basic equations in strong conservation form with the Beam-Warming approximate factorization algorithm.[6] It uses central differencing and Jameson type artificial dissipation.[7] Originally developed by Pulliam and Steger,[8] ARC was modified for propulsion analysis by Cooper[9] and accordingly named PARC. The simple rectangular inlet configuration shown in Fig. 1 was analyzed with the expectation that experimental data would be available. A flat plate of 30 in. length preceded the entrance to the inlet in order to simulate the boundary layer growth on the forebody of a hypersonic aircraft. Compression wedges form the top and bottom walls of the inlet and the contraction ratio was equal to 5. Swept sidewalls which connect the upper and lower walls prevent compressed flow from spilling over the inlet sides. Computations were made at an entrance Mach number of 12.25. Various turbulence models were used in the solutions, including those developed by McDonald-Camarata, Bushnell and Beckwith and Baldwin-Lomax. Two-dimensional PNS solutions were carried out using grids of 100 by 1000, and the three-dimensional cases used 80 by 60 by 750. The two-dimensional Reynolds averaged Navier-Stokes solutions used 100 by 200 grids whereas the three-dimensional solutions were carried out on grids of 150 by 81 by 41. Computations were performed on the Cray X-MP and the Cray 2. The PNS code described above has been modified by Liou[10] to include real gas effects. In addition, Yu et al.[11] have incorporated finite rate and local equilibrium approaches in the chemical reaction model for dissociation and ionization of the inlet air. The finite rate approach involves the simultaneous solution of eleven species equations coupled with the fluid dynamics equations. In the local equilibrium approach, a chemical equilibrium package has been developed and incorporated into the flow code to obtain chemical compositions directly. Gas properties for the reaction product species are calculated by methods of statistical mechanics and fit to a polynomial form for specific heat.

Rose and Perkins[12] have used Kumar's explicit, time-accurate implementation of MacCormack's algorithm for solving the full Navier-Stokes equations. Grid sizes used for the computations were 201 in the streamwise direction, 61 in the compression direction and 27 in the cross stream direction. Inlet surfaces were assumed to be nearly adiabatic with surface temperatures equal to stagnation temperatures.

Computed Inlet Results

Contour plots of constant Mach number within the inlet, obtained with the PNS analysis are shown in Fig. 2. The concentration of lines near the walls indicates the boundary layer, while the contour concentration in the freestream indicates shock wave locations. The flow (right to left) features seen in the figure are boundary layer buildup on the flat plate followed by thickening on the side walls and ramp surface. Shocks generated by the compression wedges are seen as horizontal lines, and the sidewall shocks as vertical lines. The shocks generated by the compression surface glance across the sidewall boundary layers, producing a thickening of the boundary in the vicinity of the shock, and thinning of the layer in the corners. Strong secondary flows are developed in the shock wave/boundary layer interaction. These flows, in turn, affect the downstream inlet flow field. A more detailed view of the flow field Mach number contours is seen in Fig. 3. In this view, which looks upstream toward the inlet entrance, the ramp and cowl compression shock waves emanating from the leading edges are clearly discernible, as well as the secondary flow developed in the corners. The boundary layer growth on the wedges and sidewalls has been highly distorted by interactions with the compression shocks. Benson et al.[4] describe their computations in the following way, which relates to the important physical processes occurring: "The low energy flow of the sidewall boundary layer has been swept up the sidewall by the ramp shock and down the sidewall by the cowl shock. Near the sidewall where the secondary flows collide, one sees a secondary shock as a vertical line. As the flow proceeds downstream to the center plane, the shock waves cross and are distorted by interaction with the sidewall boundary layer and the expansion fan on the ramp surface. At this station, the ramp shock is reflecting from the cowl surface and the cowl shock is seen as the upper horizontal line. The lower white horizontal line corresponds to the edge of the ramp boundary layer. The vortices generated by the shock/boundary layer interactions have pulled away from the sidewall while interacting with each other. Proceeding to the last plane on the left, the expansion generated on the lower surface causes a strong pressure gradient from top to bottom. Low energy flow along the sidewall moves into the corner formed by the sidewall and the ramp surface. As the shock wave created by the ramp and reflected from the cowl strikes the ramp surface, the low energy flow in the corner separates. The PNS analysis cannot be made to proceed farther due to the magnitude of the separation in the corner. At this last station, the flow is seen to be highly distorted with separation in the lower corners, vortical flow near the sidewalls and thick boundary layers on both the ramp and cowl surfaces."

An alternate visualization of the three-dimensional flow is obtained with particle tracing, as shown in Fig. 4. Computational particles were placed along the sidewall of the inlet. Interaction of the ramp and cowl shocks with the sidewall boundary layer causes the particles to converge near the shock interaction point. The particles are then displaced due to the vortex motion described earlier. Flow migration details are clearly depicted in this computational simulation. Since this vortex phenomenon persists downstream, it is proposed that judicious fuel injector design and placement may lead to enhanced mixing of air and fuel in the combustor.

Computations performed by Rose are shown in Fig. 5 for a rectangular inlet at Mach 5. The

same features shown in the previous inlet are also seen in the Mach 5 inlet, i.e., strong viscous shock effects leading to large regions of vortex flow. Rose carried out a number of numerical experiments to control the vortex phenomena in the corner regions. Figure 6 shows the baseline or no control case, followed by cowl cutback, cowl bleed and removal of a part of the sidewall. These modifications were made near the inlet ramp shoulder. It may be seen that these modifications were ineffective in eliminating the vortex region. Even with the cutback sidewall, the low momentum fluid exits along the entire sidewall. Some attenuation is seen along the cowl surface for that case. It is evident, however, that the shock-boundary layer physics within a rectangular shaped inlet will lead to pressure losses in the corner regions. However, if these regions can be utilized in an "integrated design approach," then combustor/nozzle design may benefit substantially.

Improvements Required

At the present time, the design of a low drag highly efficient inlet has not been demonstrated. It must be noted here that the geometries computed are extremely simple and, to a large extent, the computations are concentrated on developing a fundamental understanding of glancing shock/boundary layer behavior within an inlet. The results obtained yield a clear picture of the physics associated with the compression process. Observations on high speed inlets verify that the secondary flow regions do in fact occur, as predicted by the numerical code. So far, therefore, the numerical results provide realistic answers. However, real inlets are more complex in shape, may have movable geometry, will spill flow over a wide Mach number range, will probably include bleed at low Mach number flight and blowing at the higher speeds. In addition, some means for shock control and elimination of buzz and unstart will be required. A design CFD code, then, would require a full three-dimensional, time accurate Navier-Stokes code capable of handling spillage and mass addition or removal. Currently, these individual effects, such as spillage, have been computed for steady inlet flows with simplified geometries.[13] However, incorporation of all of these features into a time accurate computer code will make efficient computations all but impossible. It is worth noting that the simple geometry shown in Fig. 1 was tested and found to exhibit unsteady flow, again stressing the need for a time accurate solver. It is further noted that the issue of dispersive and dissipative errors associated with various time accurate finite-difference numerical schemes with high grid density is only now being rigorously addressed.[14] Proper boundary condition treatment is also necessary to avoid degrading the accuracy of numerical solutions. Pure acoustic radiation boundary conditions do not properly account for the effects of unsteady vortex shedding, disturbance amplification caused by separation and the response due to both vorticity oscillations and entropy waves.[14]

Up to this point, the discussion has centered on the geometric configuration of the inlet. There are also a number of problems associated with understanding the fundamental flow physics and our ability to model them. These physics are associated with the transition of the boundary layer and the nature of the turbulence modeling. Currently, there is no way to determine where the boundary layer begins to transition from laminar to turbulent, as well as the length of the transition zone. The state of the boundary layer at hypersonic speeds is unknown, and relaminarization may occur in an unpredictable manner. Direct numerical simulation may provide an approach for transition modeling at high speeds.

Reacting Flow Code

Numerical Schemes

A representative code for the analysis of combustor flow fields is described in Ref. 15. The three-dimensional code employs an implicit finite volume, lower-upper (LU) time marching method to solve the complete Navier-Stokes and species equations in a fully-coupled and efficient manner. The hydrogen-air chemistry model includes nine species and eighteen reaction steps. The code has been demonstrated for normal hydrogen injection into supersonic airstreams for nonreacting flow and also compared to other numerical schemes. The LU code, in its two-dimensional version, incorporates comprehensive real gas property models to account for high temperature flows, and includes finite rate or equilibrium chemistry. The code, RPLUS, is formulated based on eigenvalue upwinding. The scheme has the efficiency and robustness of an implicit scheme, with an operational count comparable to that of an explicit scheme. This feature of the code is of critical importance for three-dimensional calculations of a large system of equations for reacting flows. Vectorization of the code is performed by a reorganization of the indices of the grid points for parallel processing planes.

Now, we consider the case of a simple or crude combustor which utilizes some hydrogen injection from a single or double wall position into a Mach 4 freestream (see Fig. 7). For the purpose of performing computations, we assumed the temperature of the hydrogen was set at 700 K and the airstream at 1300 K. The boundary conditions include no-slip and adiabatic top wall, with gradients of variables in the streamwise direction assumed to be zero. Symmetry boundary conditions are assumed at both side walls and bottom wall. Grid sizes required for resolution of the jet interaction features were on the order of 60 by 40 by 40 (x,y,z) with clustering in both x and z for jet resolution and y clustering for boundary layer resolution. It should be re-emphasized that the case under consideration represents only a small portion of a realistic combustor geometry. In other words, this rather large computation is only a "unit problem" associated with one of the propulsion components. The results obtained with this numerical code and the grid discussed yield a great deal of the physics inherent in the injection process. Observations regarding jet interaction phenomena made over the last 20 years are accurately replicated by the code. It is noted that in the section entitled CFD Validation the ability to capture discontinuities was mentioned as one of the important numerics issues. In that regard, the recent work by Shuen and Liou[16] was directed toward a flux splitting algorithm for viscous flows with nonequilibrium chemistry. Upwind TVD differencing was used with a Roe flux splitting scheme. Nonequilibrium, frozen chemistry and idea gas assumptions were used in a sample calculation for the single jet injection case described above.

Computed Combustor Results

Figures 8 and 9 show a typical Mach number and temperature contour on yz planes for various x locations. Yu et al.[15] describe their computations in the following manner, which relates to the important physical/chemical phenomena: "Just behind the injecting orifice, the Mach number contours show a strong bow shock very close to the wall. Under the bow shock, the circular Mach number contour indicates the existence of the barrel shock structures. The jet has been bent and flows almost parallel to the primary flow. The penetration of the jet increases as the flow goes downstream. The shape of the jet also deforms as the flow goes downstream due to the presence of the streamwise vorticity in the lee of the injector. The secondary motion formed by two counter-rotating vortices gives the bent-over jet a kidney shape. In the temperature contour plots, the hottest region is along the wall because of the viscous dissipation in the high speed flow enhanced by the combustion of the H_2 and air. Away from the wall, by comparing the Mach number plots and the temperature plots, it is evident that the temperature increases after the bow shock. Further downstream a thin flame zone characterized by higher temperature is developed. Vigorous chemical reaction occurs in the flame zone." Mach number contours are also shown for the xy plane across the orifice for both the single (Fig. 10) and double jet (Fig. 11) injection computation. Features near the injection orifice(s) indicated the presence of a barrel shock structure. Separation and reattachment features upstream and downstream of the jets are also clearly discernible. In the dual injection case, blockage caused by the first jet allows the second jet to penetrate further into the free-stream due to stronger expansion. This behavior is consistent with the penetration correlation published by Povinelli et al.,[17] in that the free-stream momentum deficit approaching the jet is one of the parameters governing jet penetration.

Improvements Required

So far, we have shown that for flush, single and dual wall injection, numerical computations provide realistic answers. The results, however, cannot be extended for lengthy downstream distances with the grid resolution obtained around the jets, due to computer limitations. Hopefully, once the jet regions are computed, one could proceed with different, coarser grids downstream. Some of the general flow field property distributions would need to be passed on to the new grid. We must further consider that wall jet penetration is limited in terms of providing fuel distribution in supersonic streams. Flush wall jet penetration is on the order of 10 orifice diameters.[17] For that reason, devices like struts which span the combustor completely[18] or partially[19] are required for distribution of fuel. The numerical codes must, then, be capable of multiple wall and strut injection from many points on the solid surfaces. With partial swept struts, a typical arrangement might include 20 injection ports from the ridge line and trailing edge of each of six struts,[19] as well as selected combustor wall locations of a comparable number. Clearly, our numerical ability to perform this task is not possible. Other approaches to combustor design may be possible. For example, the possibility of enhanced mixing by the streamwise generation of vorticity has been suggested[20] and addressed in a number of ways.[21,22] Vorticity generation has been found successful for jet engine exhaust flows[23] and is currently under study at many laboratories for supersonic streams. Since most of the generation occurs through an inviscid mechanism,[23] the concept should work equally well in supersonic streams. Since it has been shown in the preceding section, Inlets, that a typical high speed inlet generates vortex flow, this flow phenomenon could be utilized as it passes downstream, to enhance combustor mixing. Vortex-shock interactions[24] and shock-shear layer interactions[25] have also been postulated for the purpose of enhanced mixing. However, these phenomena have so far proven of limited value for the improvement of mixing.

The various phenomena described above are all under continued investigation. Research on "explosive growth" in shear layer stability underway at NASA Lewis[26,27] may provide some assistance in this problem. Regardless of the understanding which will develop over the next few years, the numerical analysis will require extensive computer capabilities to handle the geometries which evolve. It is unlikely that simple combustor geometries will satisfy the requirement for this propulsion system.

So far, we have discussed the combustor geometry to a great extent. There is, however, even a greater problem associated with the fundamental phenomena of turbulent combustion and our ability to model it. Although a great deal of research has been carried out, the nature of the interaction between the fluctuating flow field and the chemical reaction steps or processes is not understood. Simple approaches related to the gross features of relatively ideal burner behavior have been made, such as flame propagation in turbulent mixtures. Those features studied have related to changes in flame speed due to increasing surface area and increasing transport but have not specifically dealt with how the flow field modifies the chemical reaction scheme. The proper modeling of turbulent flow reaction remains as a key requirement for the CFD of combustors.

For turbulent chemical reacting flows, the evaluation of the mean source (or sink) of the chemical species due to chemical reactions represents a major unsolved difficulty. The formation (or destruction) rates are nonlinear functions of temperature and species concentrations and thus knowledge of the mean-valued properties is insufficient to evaluate the mean formation rate. For example, in finite rate chemistry models, the mean formation rate calculated by using the mean-value temperature and species concentration in the Arrhenius form will lead to errors up to three orders of magnitude. Formally, the mean reaction rate could be obtained by decomposing the temperature, density, and mass fractions appearing therein into mean and fluctuating components, then taking the time (or Favre) average. The resulting equations involve many second order moments which need to be solved by extra transport equations or to be modeled. In this approach, the neglect of the correlation greater than second order terms is unsatisfactory and leads to erroneous solutions, while the retention of the higher order term renders the approach intractable.[28]

The most convenient way to circumvent this problem is to use probability density function (pdf) method. About the simplest and most popular approach is to specify a two-parameter form of the pdf in terms of mean and variance of the conserved scalar. The transport equations are readily obtained from the conservation of mass and chemical species. By solving these two equations, the pdf at each location for the whole flowfield can be obtained. Next, if the correlation is known between the conserved scalar and the chemical species concentration (which is usually calculated by equilibrium method), then the distribution of the chemical species concentration can be obtained by performing a straight forward integration. This method strongly couples the turbulence and chemical reactions. However, the choice of the pdf form and the usage of equilibrium assumption inevitably lead to errors in predicted results. There are more complex approaches along the same line, for example, the two-variable formalism adopted by Janicka and Kollmann[29] for the H_2/air flame. A single combined reaction progress variable was introduced to describe completeness of the three-body reactions while the two-body reactions are assumed to be in equilibrium. Thus the joint pdf for mixture fraction and reaction progress variable is needed to determine the thermochemical state of the flowfield.[28]

Nozzle CFD Analysis

Numerical Schemes

In order to illustrate nozzle CFD capability, a number of numerical schemes may be chosen. Ruffin et al.[30] have used a Reynolds averaged Navier-Stokes solver which contains a LDU-ADI scheme with Roe averaging and MUSCL differencing. The algorithm is diagonal in structure and requires minimal CPU per iteration. Laminar nonreacting computations of a nozzle exhaust flow field were made using two patched grids to model the geometry. The first grid consisted of 20 by 99 by 35 grid points and the second grid contained 51 by 99 by 52 grid points. Baysal et al.[31] used two Navier-Stokes numerical schemes to compute nozzle flows. Both schemes were two-dimensional. One scheme was an implicit, upwind solution and constant γ, the second scheme was an explicit MacCormack and had variable γ. Baldwin-Lomax turbulence modeling was used, and the grid dimensions were 155 by 131. Lai and Nelson[32] used the three-dimensional PARC Navier-Stokes code to compute nonaxisymmetric nozzle flows. The numerical scheme in PARC employs three point central differencing uniformly throughout the flow field to approximate spatial derivatives. Second and fourth order Jameson type artificial dissipation is included. Diagonalization of the inviscid terms simplified the block pentadiagonal system of equations to a scalar pentadiagonal system. The numerical scheme employs an ADI Beam and Warming approximate factorization. In general, the boundary conditions assume midplane spanwise symmetry, with no slip velocity and adiabatic wall temperature. For the external far field, quiescent air at normal conditions is assumed and nozzle exit plane conditions are specified. Streamwise flux gradients at the outflow boundary are assumed negligible.

Nozzle Results

Three-dimensional laminar computations by Ruffin et al.[30] were made for a flight Mach number of 7.3. The geometry chosen was that of a corresponding experimental configuration (Fig. 12). The grid zones chosen for the numerical study are shown in Fig. 13. The first grid is used for calculations up to the nozzle exit plane followed by interpolation of data to the second grid. The internal nozzle flow at the exit plane is modeled by specifying boundary layer profiles. The computed Mach number contours in the symmetry plane and the two cross-flow planes are shown in Fig. 14, with the forebody at 0°, afterbody ramp in the nozzle block region at 15°, and the long expansion plate at 20°. A complex interaction may be seen in the plume where the bow shock and the side edge vortex come together. Also, the ramp shock generated on the windward ramp causes high pressure flow to move to the leeward region. Figure 15 shows the predicted particle traces on the ramp expansion surface. In the words of Ruffin, the results are discussed in terms of the physical processes taking place: "Figure 15 (original in color) allows the identification of several flow features near the body surface. The turning of the oil traces corresponds to turning of the high pressure flow from the side edge of the ramp and above the nozzle block toward the low pressure expanded flow above the ramp. Other traces converge onto the separation line of a vortex near the side edge of the ramp. Additional traces correspond to a separation bubble at the location just after the ramp angle transitions from 15° to 20°. Finally, the footprint of the shear layer is shown by the particle traces near the far edge of the ramp. It should be noted that the predicted separation that occurs on the ramp may be induced by the assumption of laminar flow. This feature may not be present in the experimental flow field, which will be turbulent." It is noted here that Ruffin's computations were carried out in order to provide information relative to the design of a nozzle validation experiment. The proposed experimental model is fairly simple relative to an exhaust module of a NASP type vehicle. In spite of the simplicity of the model, the computed results very clearly point out the complexity of flow patterns that arise under these conditions.

In an effort to provide better definition of the nozzle flow field features, use of adaptive gridding has been studied by Hsu.[33] Figure 16 shows the Mach number contours and grid using a regular grid (Fig. 16(a) and (b)) and using an adaptive grid (Fig. 16(c) and (d)). These computations were carried out on a simple nozzle shape using a 81 by 201 regular grid. Grid adaption was carried out in the y direction only in the region above the cowl. Figure 16 shows that the use of adaptive grid yields a sharper shock and thinner boundary layer as well as diminishing the large region of shock induced boundary layer separation where the shock intersects the upper wall.

Baysal[31] also used adaptive gridding to compute the straight wall nozzle shown in Fig. 17. Again, the model is a fairly simple representation of scramjet nozzle and afterbody. Results with the implicit code are shown in Fig. 18, for nonreacting air from the nozzle and an external Mach number of 6. The nozzle/external pressure ratio was approximately 5. The shear layer can be seen originating at the cowl tip with an expansion, and it is deflected upwards at about 13°. Flow expansion proceeds down the ramp without separation. Computed values of the surface pressure on ramp

show good agreement with measured data, Fig. 19. The next calculation by Baysal[31] was carried out with the explicit code mentioned in the section Numerical Schemes, which included variable γ. The exhaust gas used was 50 percent F-12 and 50 percent argon; the free stream Mach number was 6. Density comparisons are shown in Fig. 20 and pressure contours in Fig. 19. The expansion process proceeds downstream and the shear layer deflects upwards at about 15°. The density is higher in the shear core, expanding back to its upstream value. Separation on the external cowl surface occurs, extending a significant distance upstream.

The computations of Lai and Nelson[32] were carried out for the nozzle experimental geometry of Re and Leavitt.[34] The geometry is shown in Fig. 21, and the nozzle exhaust grids used are shown in Fig. 22. The spanwise grid distribution is shown in Fig. 23. A three-dimensional computation was carried out matching the nozzle operating conditions which exhaust into still air. Streamwise contours for Mach number are shown at four different spanwise positions in Fig. 24. Figure 24(a) shows the contours at the nozzle mid-plane, and Figs. 24(b) to (d) move progressively outward to the nozzle sidewall. Behavior of the shear layer formed on the three-dimensional surface of the jet is clearly evident, as one scans Figs. 24 and 25 which are the cross-sectional planes in the x or downstream direction. The shear layer is observed to be highly three-dimensional in its structure with significant variations from top wall to bottom wall to side wall. Comparisons of the computed wall pressure with experimental data, Fig. 26, show good agreement for both surfaces.

Improvements Required

In all of the cases described so far, the nozzle entrance flow field was uniform and nonreacting. In a scramjet module, the combustor and nozzle are very closely coupled which means that nonuniformities in temperature, pressure and species concentration will be present at the nozzle entrance. The sensitivity of the nozzle configuration to these nonuniformities has been a matter of debate for some time. It has been proposed by this author that three-dimensional reacting nonuniform profiles should be used in CFD codes to determine the performance sensitivity of the nozzle. In this way, it would be possible to determine what profiles are desirable at the nozzle entrance for high performance. The knowledge of those profiles would provide combustor designers with "targets" or goals to achieve at the combustor exit plane in terms of pressure, temperature and concentrations. A start on providing an answer to this approach has been initiated by Tsai and Yu[35] who performed three-dimensional Navier-Stokes computations for a reacting hydrogen-air mixture as well as for frozen flow. Using a numerical scheme based on the LU approach of Yoon and Jameson,[36] pressure, temperature and Mach number distributions for both flow solutions have been compared as well as the OH, O and H mass fraction distributions. Calculation of the relative nozzle thrusts in a typical non axisymmetric configuration is still required in order to support the proposal made by this author. The ability to compute multi-exhaust modules integrated into a realistic aftbody with reacting flow exhaust over a wide Mach number range has not yet been demonstrated.

Flow separation at transonic speeds will cause significant drag losses. To date, no realistic simulation of the transonic regime has been performed. Separation of the external cowl boundary layer and incorporation of means to prevent the separation also have not been simulated. Prevention methods could include burning or deployment of a wall section such as in the aftbody. As in the other components, turbulence and transition modeling remain as significant unknowns. Relaminarization of the aftbody boundary layer is also a phenomenon which could occur. Heat transfer to the aftbody is also a computational issue which requires a significant amount of attention.

Conclusions

Based on the results presented in this paper, it is evident that there are many portions or features of a hypersonic propulsion system that have not been properly or accurately simulated by numerical analyses. The inlet behavior and its performance for both steady and unsteady operation have been computed for fairly simple geometries, and none of the computations incorporates all of the physics which are known to occur. The design of a high efficiency supersonic inlet, designed for a relatively narrow Mach number range, is not a simple design matter. High recovery, reduced heat load, proper cowl lip design and low spillage drag are all required while delivering usable exit profile conditions to the combustor. In the spirit of a totally integrated propulsion system design, the features of the inlet flow field must be considered as part of the combustor/nozzle design. Some thoughts on the utilization of inlet flow features for combustor design were presented in this paper. It is noted, finally, that unsteady inlet behavior with mass addition and flow spillage must be properly simulated by numerical methods in order to establish a reliable design.

In the combustor region, it is clear that only crude design features have been modeled and computed. Realistic geometries, incorporating struts, wedges and wall injection must be computed in order to provide any design benefits. Aside from the additional geometric complexity needed, the fundamental nature of turbulence-combustion interaction remains as a major unknown. The proper modeling of the unsteady flow field, both random and deterministic, with the combustion chemistry remains a major challenge. PDF modeling appears to be one of the promising avenues to pursue in this regard.

Nozzle flows are characterized by intricate patterns of shock waves and shear layers. The asymmetry of the nozzle, combined with the shear layer position, reflect the shocks in various directions. Shear layer bending occurs at the shock intersection locations. The shape and structure of these features vary considerably over the flight Mach number range with the attendant changes in nozzle back pressure. Much remaining work needs to be performed on the expansion of reacting gases with properly modeled entrance profiles of both flow stream aero properties and concentration profiles. It has been suggested in this paper that the efficient design of a hypersonic nozzle should proceed by exploring the best profiles for optimum nozzle performance. Those profiles then provide a goal for combustor exit conditions. Further deficiencies in the nozzle area are associated with

nonexistent modeling for reacting separated flow. Numerical prediction of the state of the boundary layer is also not feasible. In addition, accurate heat transfer computations for the nozzle wall have yet to be demonstrated over the range of operating conditions. In closing, it is important to note that real gas and thermal and chemical nonequilibrium effects must be considered in all of the propulsion system components at the appropriate flight conditions.

Advances in two other areas are required. The first advance involves the further development of accurate and efficient numerical methods required to improve solution accuracy with an attendant reduction in computing time. The second advance relates to computer technology and includes issues of speed, storage, structure and graphics.

It is not the intent of this paper to present the opinion that a realistic computer simulation for a hypersonic vehicle poses an impossible task. Rather the intent is to assess, in as realistic a fashion as possible, what is achievable with todays knowledge, numerical codes and computers. The progress in these areas has been remarkable over the last decade and will continue to be so in the future. It is with this understanding that this author is confident that a complete simulation over the entire flight range will be possible someday. However, the progression of the simulations to the point where design type information can be obtained, such as described earlier (Propulsion CFD Validation section), can only occur if the validation process is carried forward with more realistic propulsion geometries.

References

1. Dwoyer, D.L., Kutler, P., and Povinelli, L.A., "Retooling CFD for Hypersonic Aircraft," Aerospace America, Vol. 25, Oct. 1987, pp. 32-35,41.

2. Benson, T.J., "Three-Dimensional Viscous Calculation of Flow in a Mach 5.0 Hypersonic Inlet," AIAA Paper 86-1461, June 1986.

3. Kunik, W.G., Benson, T.J., Ng, W.-F., and Taylor, A., "Two- and Three-Dimensional Viscous Computations of a Hypersonic Inlet Flow," AIAA Paper 87-0283, Jan. 1987.

4. Reddy, D.R., Smith, G.E., Liou, M.-F., and Benson, T.J., "Three Dimensional Viscous Analysis of a Hypersonic Inlet," AIAA Paper 89-0004, Jan. 1989. (See also NASA TM-101474.)

5. Kim, Y.N., Buggeln, R.C., and McDonald H., "Numerical Analysis of Some Supersonic Viscous Flows Related to Inlet and Nozzle Systems," AIAA Paper 86-1597, June 1986.

6. Beam, R.M., and Warming, R.F., "An Implicit Factored Scheme for the Compressible Navier-Stokes Equations," AIAA Journal, Vol. 16, No. 4, April 1978, pp. 393-402.

7. Jameson, A., and Baker, T.J., "Solution of the Euler Equations for Complex Configurations," AIAA Paper 83-1929, July 1983. (See also Computational Fluid Dynamics, 6th, New York, AIAA, pp. 293-302.)

8. Pulliam, T.H., and Steger, J.L., "Implicit Finite-Difference Simulations of Three-Dimensional Compressible Flow," AIAA Journal, Vol. 18, No. 2, Feb. 1980, pp. 159-167.

9. Cooper, G.K., Jordan, J.L., and Phares, W.J., "Analysis Tool for Application to Ground Testing of Highly Underexpanded Nozzles," AIAA Paper 87-2015, July 1987.

10. Liou, M.-F., "Three Dimensional PNS Solutions of Hypersonic Internal Flows with Equilibrium Chemistry," AIAA Paper 89-0002, Jan. 1989.

11. Yu, S.-T., McBride, B.J., Hsieh, K.-C., and Shuen, J.-S., "Numerical Simulation of Hypersonic Inlet Flows with Equilibrium or Finite Rate Chemistry," AIAA Paper 88-0273, Jan. 1988.

12. Rose, W.C., and Perkins, E.W., "Innovative Boundary Layer Control Methods in High Speed Inlet Systems-Final Report," Contract NAS3-25408, Sept. 9, 1988. (NASA CR in publication.)

13. Narayan, J., and Kumar, A., "A Numerical Study of Hypersonic Propulsion/Airframe Integration Problem," AIAA Paper 89-0030, Jan. 1989.

14. Hsieh, K.-C., "An Assessment of Numerical Techniques for Unsteady Flow Calculations," AIAA CFD Conference, Buffalo, New York, June 1989.

15. Yu, S.-T., Tsai, and Shuen, J.-S., "Three-Dimensional Solution of Subsonic Reacting Flows with Finite Rate Chemistry," AIAA Paper 89-0391, Jan. 1989.

16. Shuen, J.-S. and Liou, M.-S., "Flux Splitting Algorithms for Two-Dimensional Real Gas Flows," AIAA Paper 89-0388, Jan. 1989.

17. Povinelli, F.P., and Povinelli, L.A., "Correlation of Secondary Sonic and Supersonic Gaseous Jet Penetration into Supersonic Crossflows," NASA TN-D-6370, June 1971.

18. Anderson, G.Y., and Gooderum, P.B., "Exploratory Tests of Two Strut Fuel Injectors for Supersonic Combustion," NASA TN-D-7581, Feb. 1974.

19. Povinelli, L.A., "Aerodynamic Drag and Fuel Spreading Measurements in a Simulated Scramjet Combustion Module," NASA TN-D-7674, May 1974.

20. Povinelli, L.A., Povinelli, F.P.; and Hersch, M., "A Study of Helium Penetration and Spreading in a Mach 2 Airstream Using a Delta Wing Injector," NASA TN-D-5322, July 1969.

21. Hersch, M., and Povinelli, L.A., "Effect of Interacting Vortices on Jet Penetration into a Supersonic Stream," NASA TM-X-2134, Nov. 1970.

22. Marble, F.E., Hendricks, G.J., and Zukoski, E.E., "Progress Toward Shock Enhancement of Supersonic Combustion Processes," AIAA Paper 87-1880, June 1987.

23. Povinelli, L.A., and Anderson, B.H., "Investigation of Mixing in a Turbofan Exhaust Duct, Part II: Computer Code Application and Verification," AIAA Journal, Vol 22, No. 4, April 1984, pp. 518-525.

24. Povinelli, L.A., and Ehlers, R.C., "Swirling Base Injection for Supersonic Combustion Ramjets," AIAA Journal, Vol. 10, No. 9, Sept. 1972, pp. 1243-1244.

25. Menon, S., "Shock Wave-Induced Enhanced Mixing in Scramjet Combustor," AIAA Paper 89-0104, Jan. 1989.

26. Goldstein, M.E., and Lieb, S.J., "Non-Linear Evolution of Oblique Waves on Compressible Shear Layers," Journal of Fluid Mechs., to be published in 1989.

27. Balsa, T.F., and Goldstein, M.E., "On the Instabilities of Supersonic Mixing Layers: A High Mach Number Asymptotic Theory," Journal of Fluid Mechs., to be published in 1989.

28. Yu, Sheng-Tao, personal communication, NASA Lewis Research Center, Cleveland, OH.

29. Janicka, J., and Kollmann, W., "A Prediction Model for Turbulent Diffusion Flames Including NO-Formation," Combustor Modelling--AGARD-CP-275, 1980.

30. Ruffin, S.M., Venkatopathy, E., Keener, E.R., and Nagaraj, N., "Computational Design Aspects of a NASP Nozzle/Afterbody Experiment," AIAA Paper 89-0446, Jan. 1989.

31. Baysal, O., Engelund, W.C., Eleshaky, M.E., and Pittman, J.L., "Adaptive Computations of Viscous Scramjet-Afterbody Flows With and Without Multi-species," AIAA Paper 89-0009, Jan. 1989.

32. Lai, H., and Nelson, E., "Comparison of 3D Computation and Experiment for Non-Axisymmetric Nozzles," AIAA Paper 89-0007, Jan. 1989.

33. Hsu, A.T., "The Effect of Adaptive Grid on Hypersonic Nozzle Flow Calculations," AIAA Paper 89-0006, Jan. 1989.

34. Re, R.J., and Leavitt, D.L., "Static Internal Performance of Single-Expansion-Ramp Nozzles with Various Combinations of Internal Geometric Parameters," NASA TM-86270, Dec. 1984.

35. Tsai, Y.-L.P., and Yu, S.-T., "Chemically Reacting Flow Calculations for Nozzles Using an LU Scheme in Three Dimensions," AIAA/ASME/SAE/ASEE 25th Joint Propulsion Conference, July 1989.

36. Yoon, S., and Jameson, A., "An LU-SSOR Scheme for the Euler and Navier-Stokes Equations," AIAA Paper 87-0600, Jan. 1987.

Table 1. - Forebody Requirements

Performance parameters
Lift
Drag
Heat load
Inlet profiles
Computed variables required
Pressure
Skin friction
Heat transfer
Inlet profiles (u,v,w,p,T,C_i)
Integrals for performance
Physical/chemical modeling requirements
Transition
Turbulence
Shock boundary layer interactions
Vortical flow
Entropy layer swallowing
Equilibrium, nonequilibrium chemistry
Wall catalyticity
Low density flow

Table 2. - Inlet Requirements

Performance parameters
Mass capture
Kinetic energy efficiency
Pressure recovery
Heat load
Exit profiles to combustor
Computed variables required
Wall pressure
Skin friction
Heat transfer
Exit profiles (u,v,w,T,C_i)
Physical/chemical modeling requirements
Shock boundary layer interactions
Secondary/corner flows
Mass injection
Low Mach number bleed
Flow separation
Shock induced unsteadiness
Turbulence, transition
Equilibrium chemistry
Flow unsteadiness

Table 3. - Combustor Requirements

Performance parameters
Thrust
Heat load
Combustion efficiency
Pressure losses
Structural load
Computed variables required
Wall pressure
Heat transfer
Skin friction
Exit profiles (u,v,w,T,C_i)
Physical/chemical modeling requirements
Finite rate chemistry
Shock interactions
Shear layers
Vortex/shock interactions
Heat transfer
Injector interactions
Turbulence

Table 4. - Nozzle Requirements

Performance parameters
Thrust
Moment
Heat load
Computed variables required
Wall pressure
Heat transfer
Skin friction
Physical/chemical modeling requirements
Finite rate chemistry
Turbulence
Shock interactions
Shear layers
Secondary flows
Separation
Relaminarization

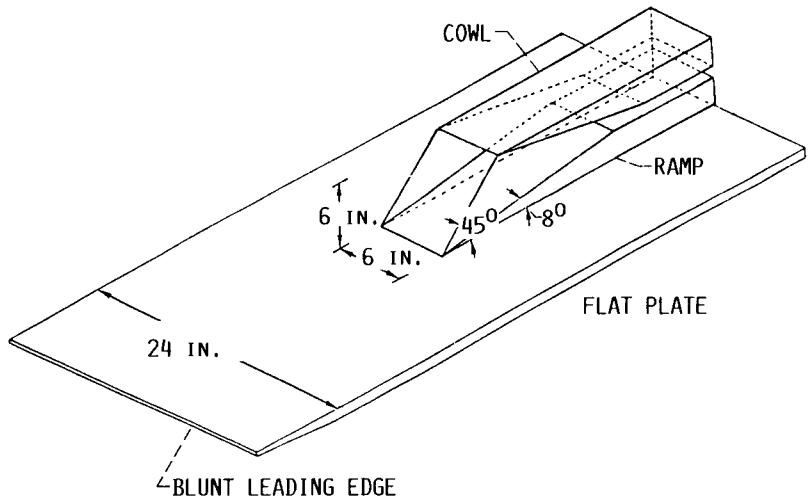

FIGURE 1. - EXPERIMENTAL MACH 12 INLET GEOMETRY (REF. 4).

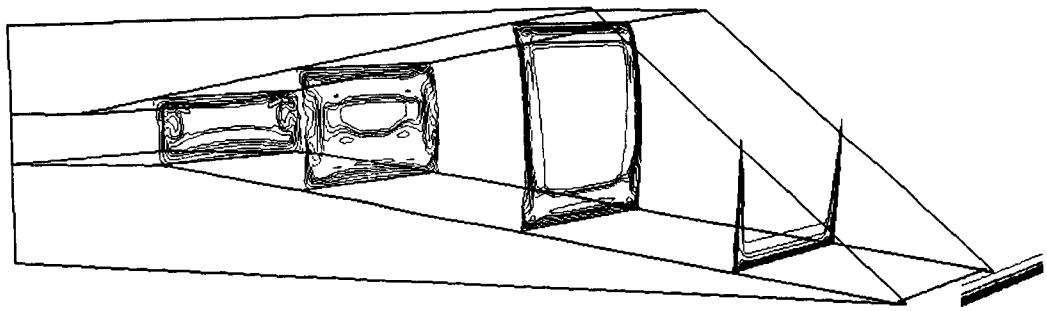

FIGURE 2. - MACH NUMBER CONTOURS, M = 12.25 (REF. 4).

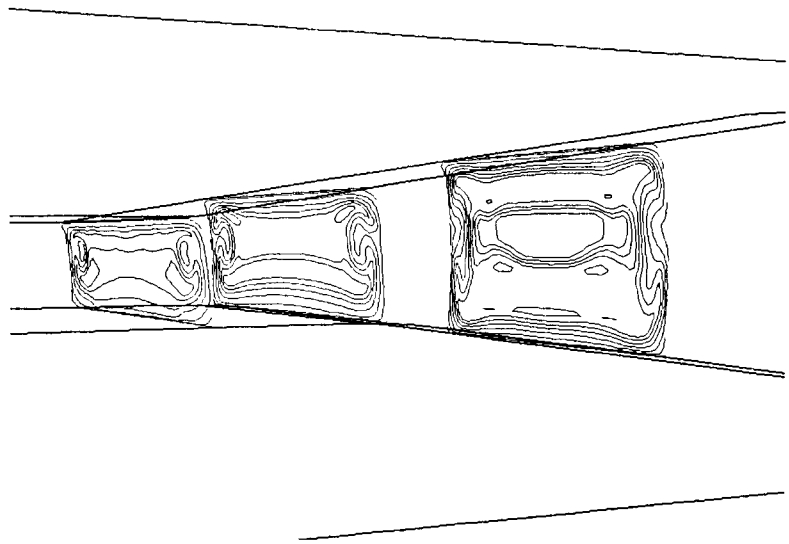

FIGURE 3. - MACH NUMBER CONTOURS VIEWED FROM AFT (REF. 4).

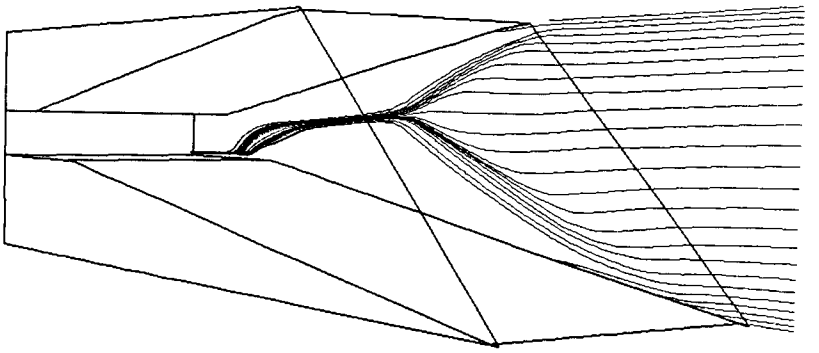

FIGURE 4. - SIDEWALL PARTICLE TRACING, M = 12.25 (REF. 4).

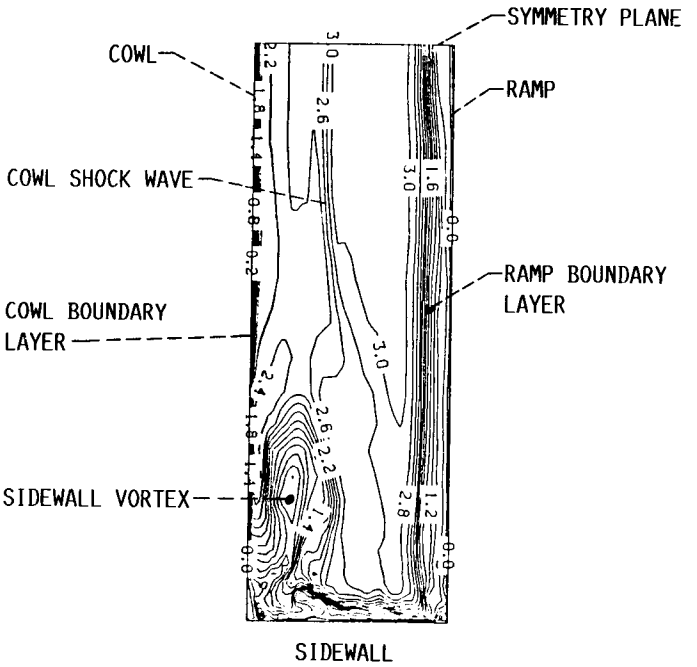

FIGURE 5. - ORIENTATION OF CROSSFLOW PLANE 150 LOCATED NEAR THE RAMP SHOULDER SHOWING PLANE OF SYMMETRY, SIDEWALL RAMP AND COWL SURFACES (REF. 12).

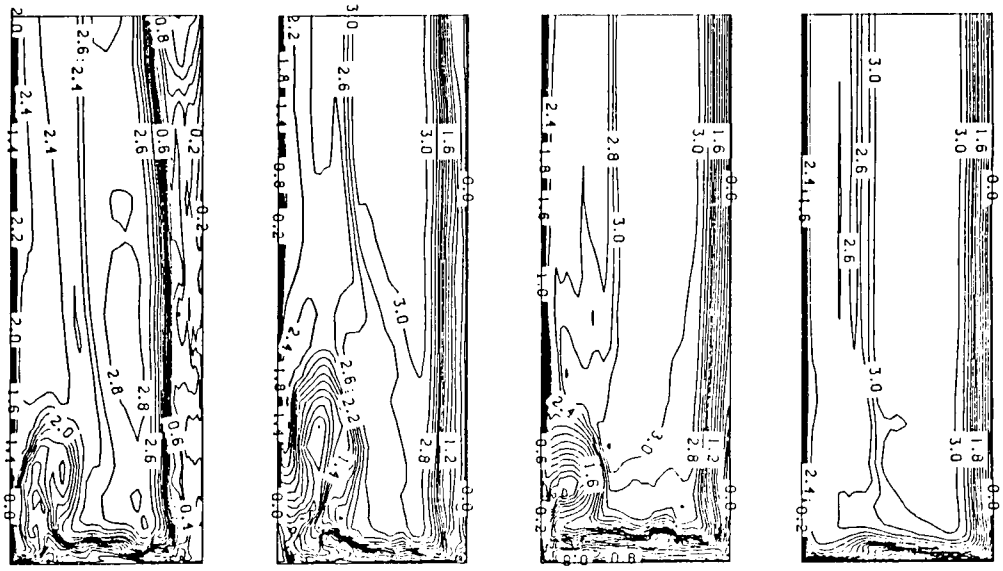

NO CONTROL CUTBACK COWL COWL BLEED CUTBACK SIDEWALL

FIGURE 6. - COMPARISON OF EFFECT OF VARIOUS CONTROL METHODS ON MACH NUMBER CONTOURS NEAR RAMP SHOULDER (REF. 12).

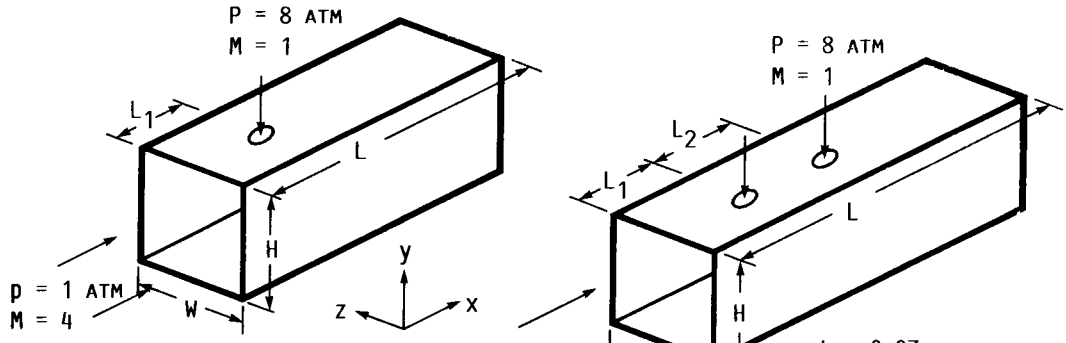

FIGURE 7. - FLOW CONFIGURATIONS (REF. 15).

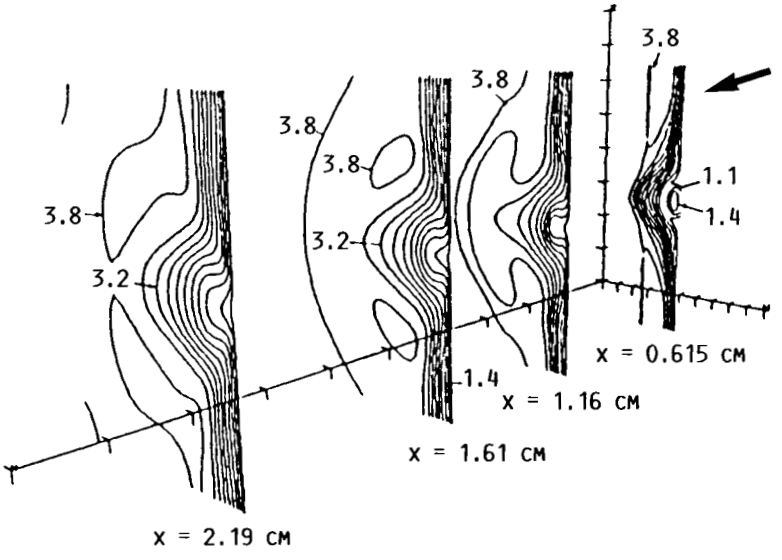

FIGURE 8. - MACH NUMBER CONTOURS ON yz PLANES AT VARIOUS x LOCATIONS FOR CASE 1 (REF. 15).

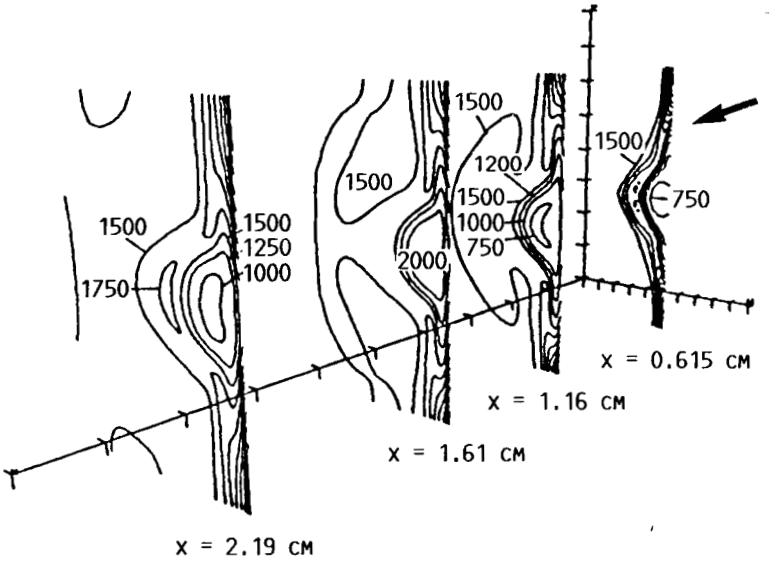

FIGURE 9. - TEMPERATURE CONTOURS ON yz PLANES AT VARIOUS x LOCATIONS FOR CASE 1 (REF. 15).

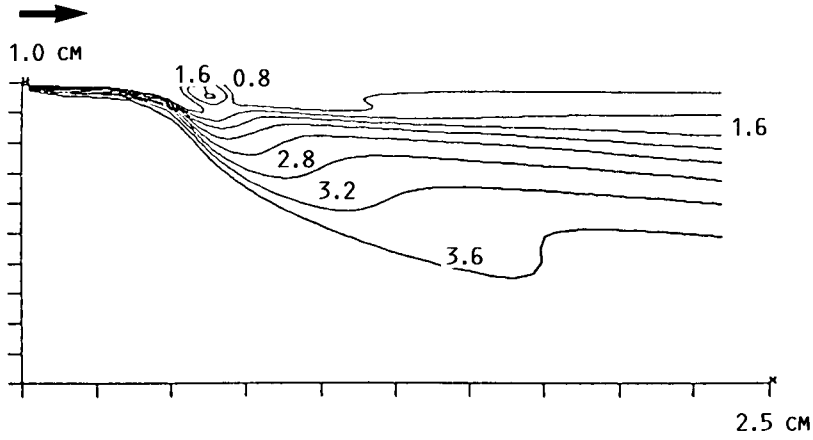

FIGURE 10. - MACH NUMBER CONTOUR ON xy PLANE AT CENTER OF INJECTION PORT FOR CASE 1 (REF. 15).

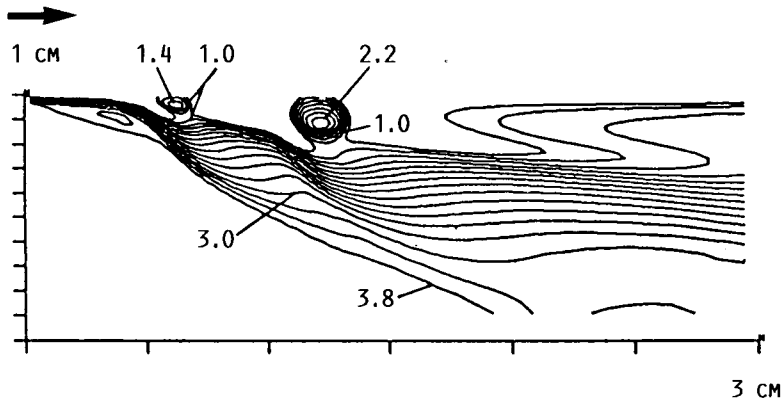

FIGURE 11. - MACH NUMBER CONTOUR ON xy PLANE AT CENTER OF INJECTION PORT FOR CASE 2 (REF. 15).

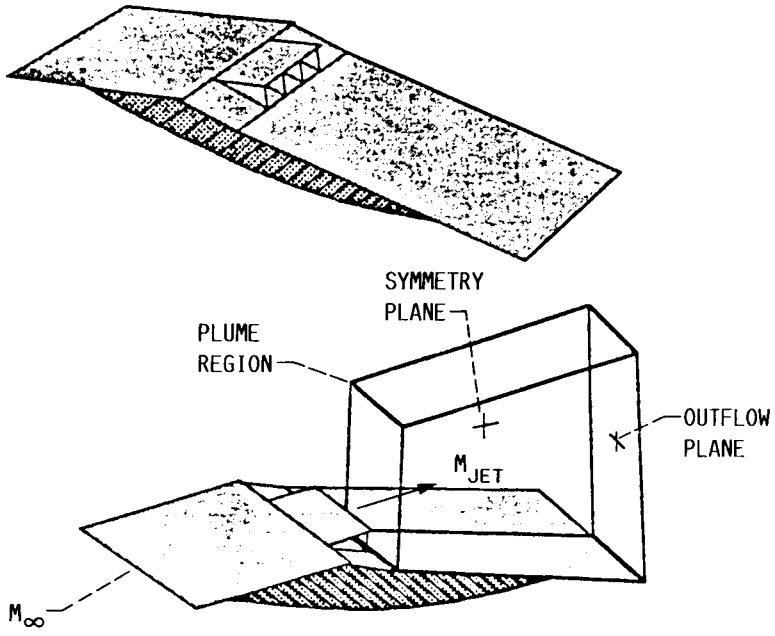

FIGURE 12. - SCHEMATIC OF EXPERIMENTAL MODEL, PERSPECTIVE VIEWS (REF. 30).

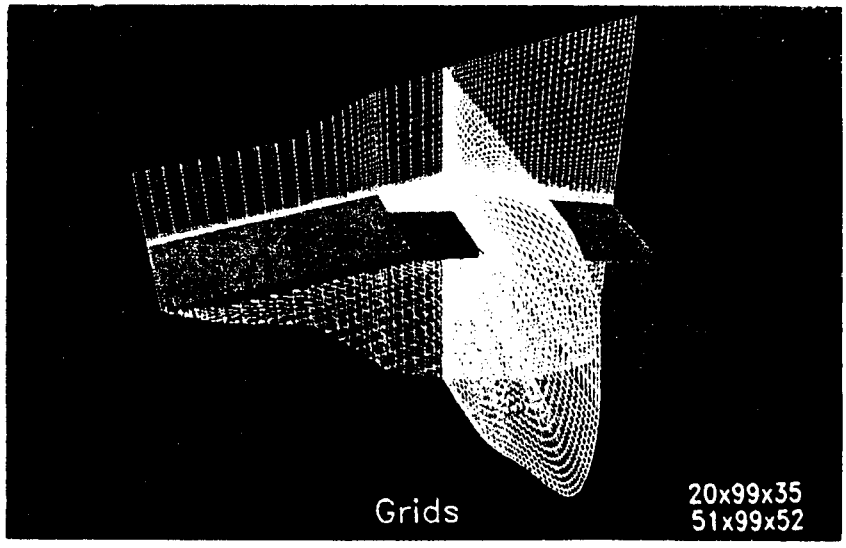

FIGURE 13. - GRID SYSTEM PERSPECTIVE VIEW FOR 3-D COMPLETE GEOMETRY CALCULATION, CASE-1, $\alpha_r = 20^0$ (REF. 30).

FIGURE 14. - MACH CONTOUR PERSPECTIVE VIEW FOR 3-D COMPLETE GEOMETRY CALCULATION, CASE-1, $\alpha_r = 20^0$ (REF. 30).

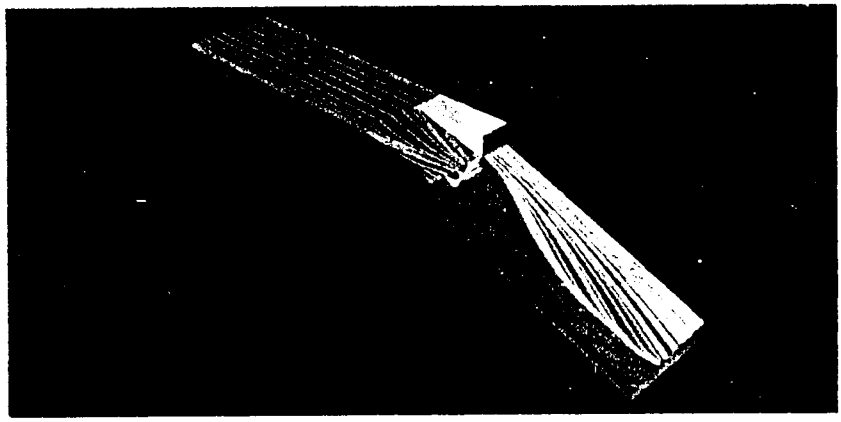

FIGURE 15. - SIMULATED SURFACE OIL FLOW FOR 3-D COMPLETE GEOMETRY CALCULATION, CASE-1, $\alpha_r = 20^0$ (REF. 30).

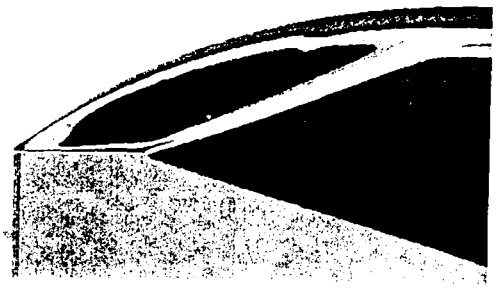

(a) SOLUTION ON A REGULAR GRID.

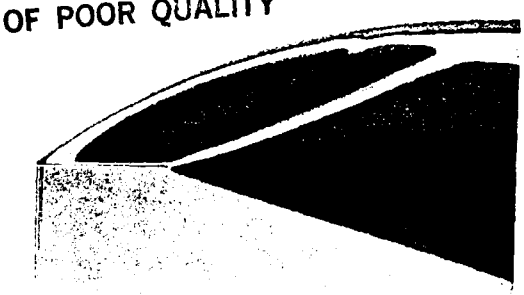

(c) SOLUTION ON AN ADAPTIVE GRID.

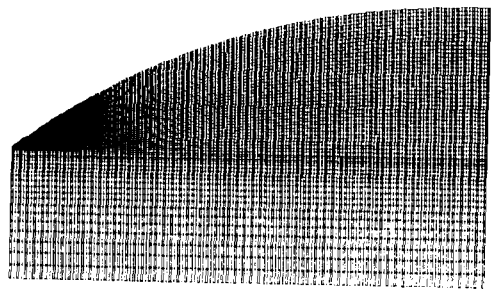

(b) NONADAPTIVE GRID FOR NOZZLE FLOW.

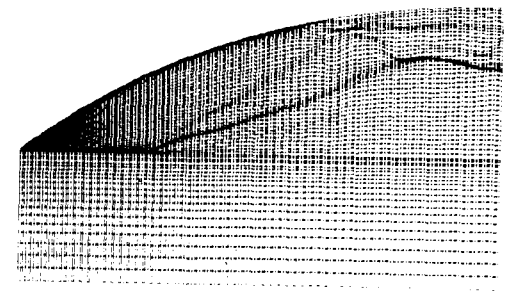

(d) ADAPTIVE GRID FOR NOZZLE FLOW.

FIGURE 16. - MACH NUMBER CONTOURS AND GRIDS FOR A SCRAMJET NOZZLE (REF. 33).

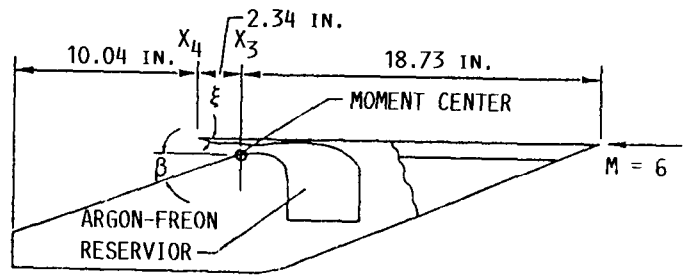

(a) SECTIONAL VIEW.

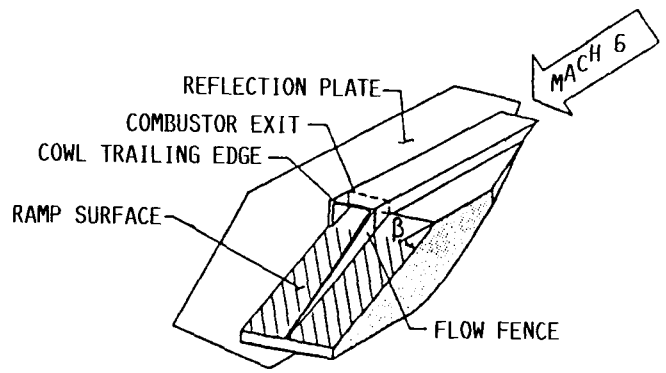

(b) ISOMETRIC VIEW.

FIGURE 17. - MODEL OF AFTERBODY WITH SCRAMJET EXHAUST SIMULATION (REF. 31).

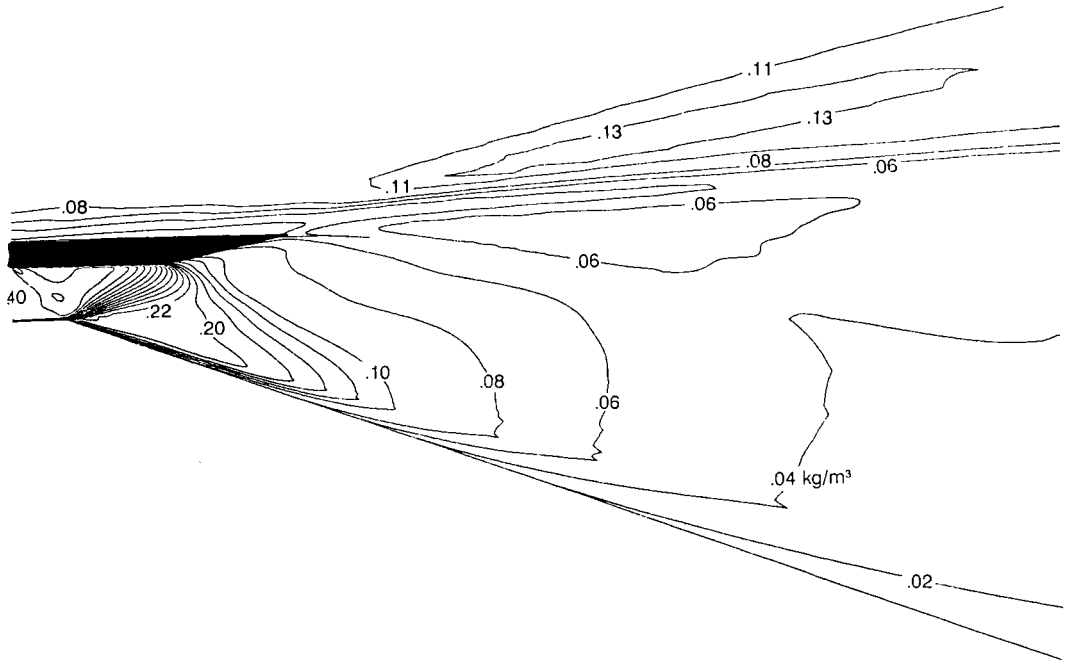

FIGURE 18. - DENSITY CONTOURS FOR CASE 2 (REF. 31).

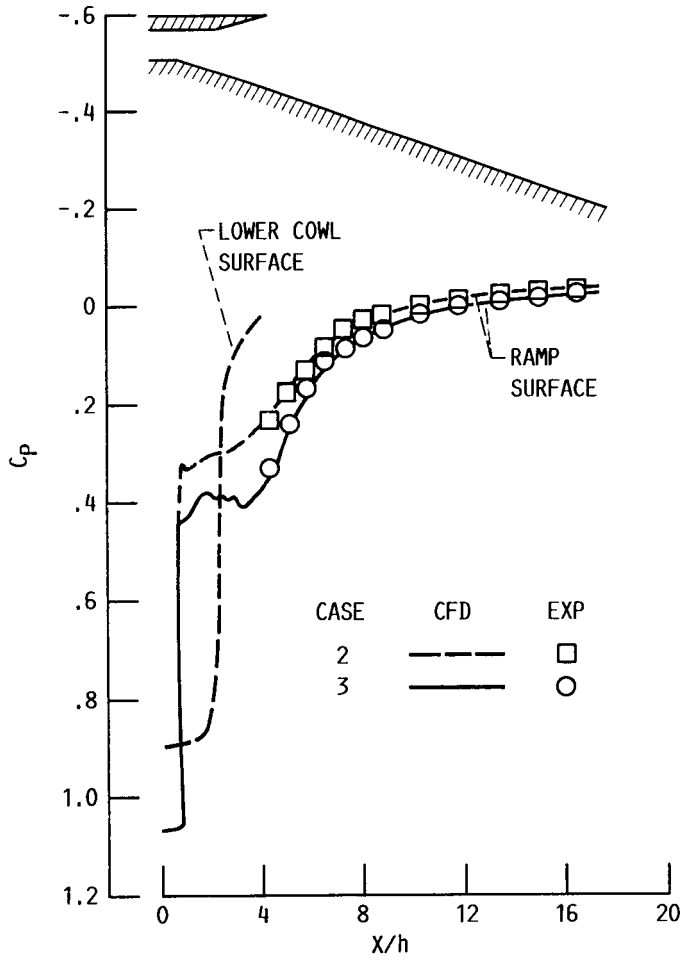

FIGURE 19. - PRESSURE COEFFICIENT DISTRIBUTIONS ON RAMP AND LOWER COWL SURFACES (REF. 31).

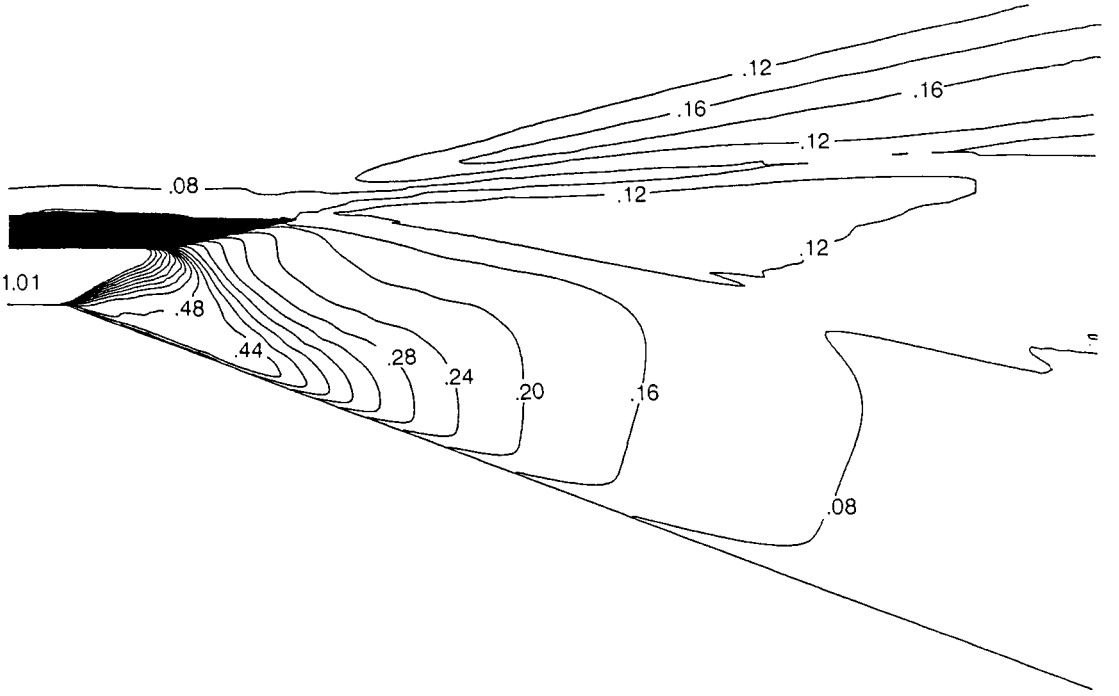

FIGURE 20. - DENSITY CONTOURS FOR CASE 3 (REF. 31).

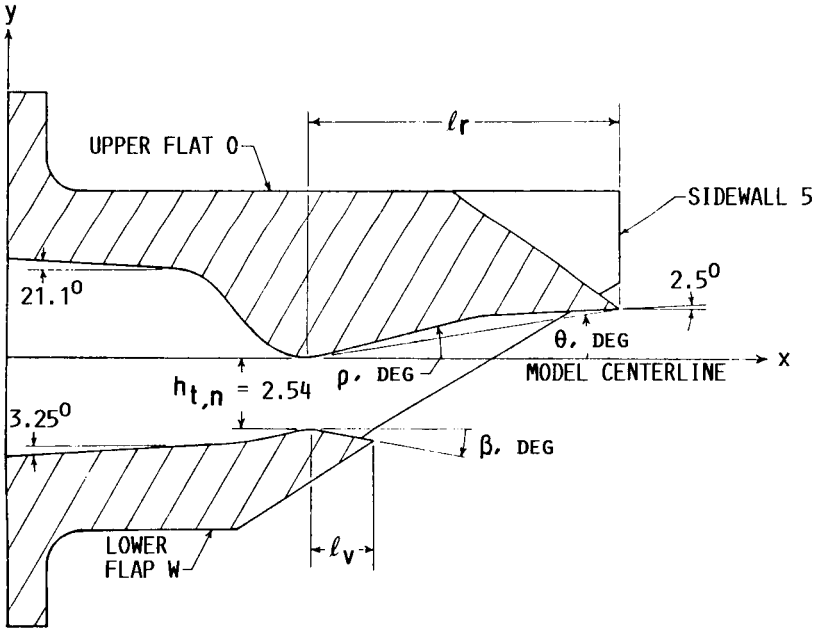

FIGURE 21. - NOZZLE GEOMETRY (REF. 32).

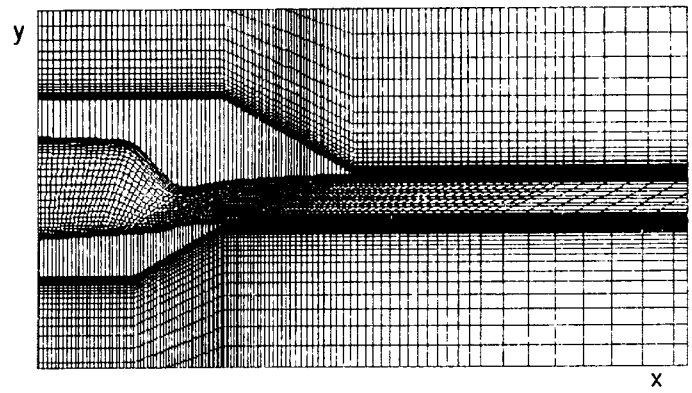

(a) NOZZLE AND EXHAUST GRID.

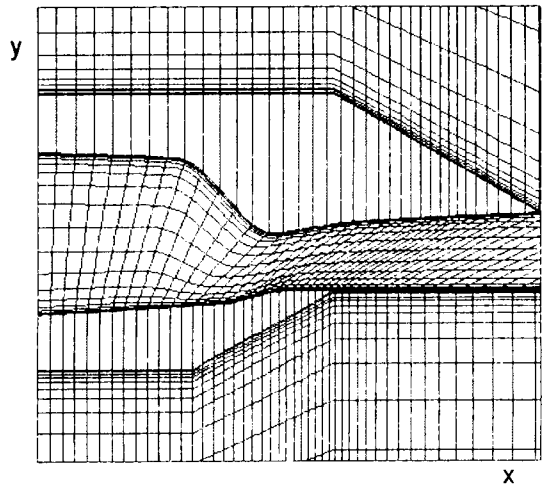

(b) NOZZLE GRID.

FIGURE 22. - STREAMWISE GRID DISTRIBUTION (REF. 32).

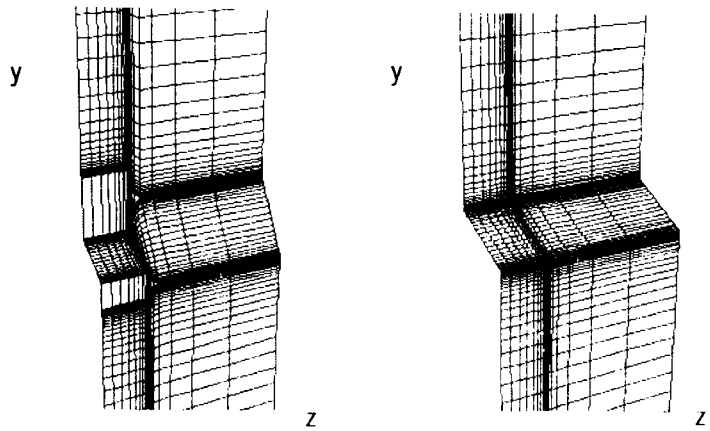

(a) IN THE NOZZLE REGION. (b) IN THE EXHAUST REGION.

FIGURE 23. - SPANWISE GRID DISTRIBUTION (REF. 32).

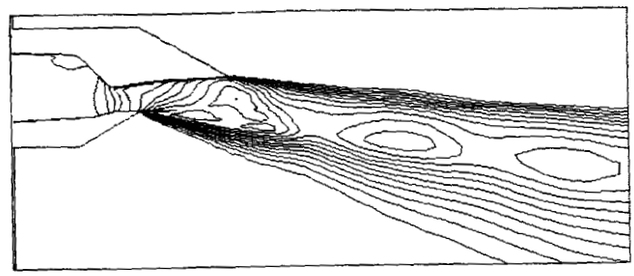

(a) I = 1, z = 0.

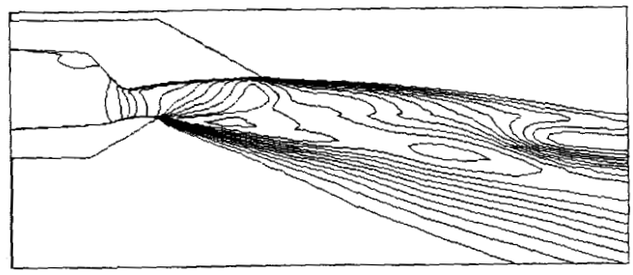

(b) I = 9, z = 1.365.

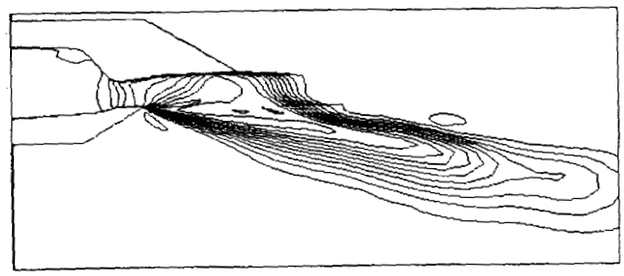

(c) I = 13, z = 1.7.

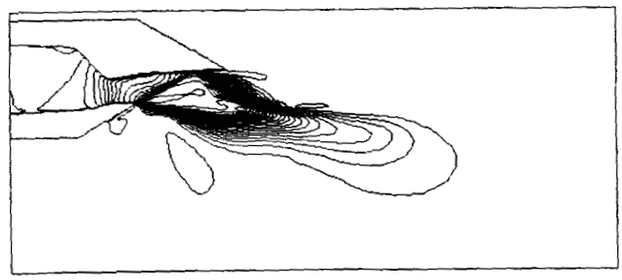

(d) I = 25, z = 1.982.

FIGURE 24.- STREAMWISE MACH NUMBER CONTOURS, CASE 1 (REF. 32).

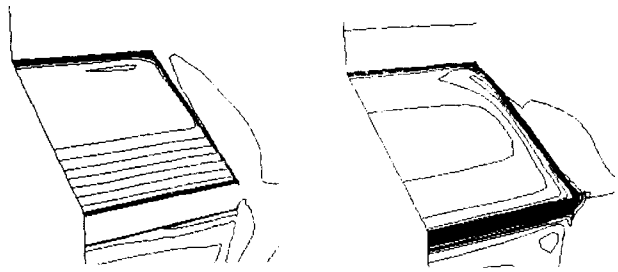

(a) i = 50, x = 4.485. (b) i = 65, x = 5.372.

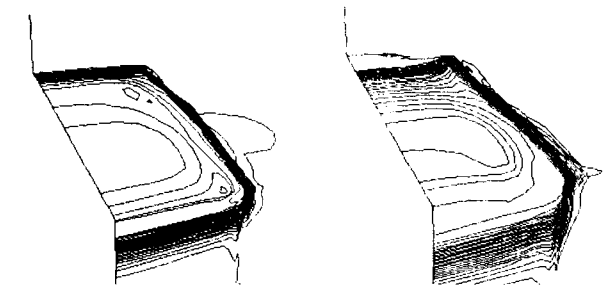

(c) i = 75, x = 6.221. (d) i = 85, x = 7.513.

FIGURE 25. - SPANWISE MACH NUMBER CONTOURS, CASE 1 (REF. 32).

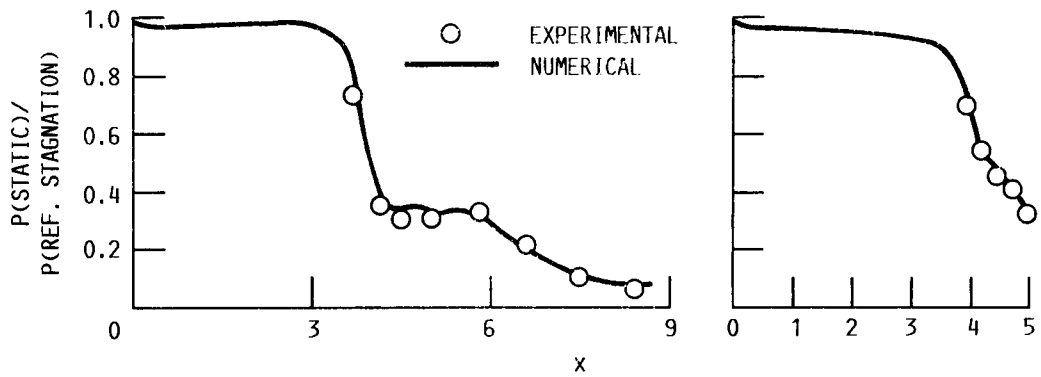

(a) UPPER WALL. (b) LOWER WALL.

FIGURE 26. - WALL PRESSURE DISTRIBUTIONS, CASE 1 (REF. 32).

NASA
National Aeronautics and Space Administration

Report Documentation Page

1. Report No.	2. Government Accession No.	3. Recipient's Catalog No.
NASA TM-102005		

4. Title and Subtitle	5. Report Date
Advanced Computational Techniques for Hypersonic Propulsion	6. Performing Organization Code

7. Author(s)	8. Performing Organization Report No.
Louis A. Povinelli	E-4711
	10. Work Unit No. 505-62-21

9. Performing Organization Name and Address	11. Contract or Grant No.
National Aeronautics and Space Administration Lewis Research Center Cleveland, Ohio 44135-3191	13. Type of Report and Period Covered Technical Memorandum

12. Sponsoring Agency Name and Address	14. Sponsoring Agency Code
National Aeronautics and Space Administration Washington, D.C. 20546-0001	

15. Supplementary Notes

Prepared for the 9th International Symposium on Air Breathing Engines cosponsored by the American Institute of Aeronautics and Astronautics and the International Society for Air Breathing Engines, Athens, Greece, September 4-9, 1989.

16. Abstract

CFD has played a major role in the resurgence of hypersonic flight, on the premise that numerical methods will allow us to perform simulations at conditions for which no ground test capability exists. Validation of CFD methods is being established using the experimental data base available, which is below Mach 8. It is important, however, to realize the limitations involved in the extrapolation process as well as the deficiencies that exist in numerical methods at the present time. Current features of CFD codes are examined for application to propulsion system components. The shortcomings in simulation and modeling are identified and discussed.

17. Key Words (Suggested by Author(s))	18. Distribution Statement
CFD Hypersonic propulsion Numerical methods Propulsion CFD	Unclassified – Unlimited Subject Category 34

19. Security Classif. (of this report)	20. Security Classif. (of this page)	21. No of pages	22. Price*
Unclassified	Unclassified	24	A03

NASA FORM 1626 OCT 86

*For sale by the National Technical Information Service, Springfield, Virginia 22161